NIH Public Access
Author Manuscript
*J Biomol Screen*. Author manuscript; available in PMC 2013 April 03.

Published in final edited form as:
*J Biomol Screen*. 2012 August ; 17(7): 885–899. doi:10.1177/1087057112446174.

# A High-Content Biosensor Based Screen Identifies Cell Permeable Activators and Inhibitors of EGFR Function: Implications in Drug Discovery

**Christophe Antczak**, **Jeni P. Mahida**, **Bhavneet Bhinder**, **Paul A. Calder**, and **Hakim Djaballah**[*]
HTS Core Facility, Molecular Pharmacology & Chemistry Program, Memorial Sloan-Kettering Cancer Center, 1275 York Avenue, New York, NY 10065, USA

## Abstract

Early success of kinase inhibitors has validated their use as drugs. However, discovery efforts have also suffered from high attrition rates; due to lack of cellular activity. We reasoned that screening for such candidates in live cells would identify novel cell permeable modulators for development. For this purpose, we have used our recently optimized EGFR biosensor (EGFRB) assay to screen for modulators of EGFR activity. Here, we report on its validation under HTS conditions displaying a S/N ratio of 21 and a Z' value of 0.56; attributes of a robust cell based assay. We performed a pilot screen against a library of 6,912 compounds demonstrating good reproducibility and identifying 82 inhibitors and 66 activators with initial hit rates of 1.2% and 0.95 %, respectively. Follow up dose response studies revealed that 12 out of the 13 known EGFR inhibitors in the library confirmed as hits. ZM-306416, a VEGFR antagonist, was identified as a potent inhibitor of EGFR function. Flurandrenolide, beclomethasone and ebastine were confirmed as activators of EGFR function. Taken together, our results validate this novel approach and demonstrate its utility in the discovery of novel kinase modulators with potential use in the clinic.

### Keywords

EGFR; domain-based biosensor; high content analysis; live cell imaging

## INTRODUCTION

The critical role of protein phosphorylation in the development and progression of many cancers has driven considerable efforts to discover therapeutic agents targeting aberrant signaling events. Receptor Tyrosine Kinases (RTKs) such as EGFR play a well established role in several cancers and have become a crucial class of targets for the development of small molecule anticancer agents.[1] Besides high-profile successes such as Iressa (gefitinib) and Tarceva (erlotinib), progress in identifying new drugs inhibiting RTKs has been slow in recent years. A major obstacle hampering the rapid discovery of new effective drugs inhibiting RTKs is the lack of cellular activity of potent and selective candidates originally identified in screens relying on assays using recombinant kinase domains. Such RTK inhibitors very often fail the transition from being potent toward purified recombinant protein to being active in cells, believed to be due to mainly to lack of cellular permeability. As a consequence, time-consuming exploratory chemistry efforts are needed to enhance the

[*]**Corresponding author:** Hakim Djaballah, PhD. Director, HTS Core Facility, MSKCC, NY, USA. djaballh@mskcc.org; Tel (646) 888-2198..

NIH-PA Author Manuscript
NIH-PA Author Manuscript
NIH-PA Author Manuscript

NIH-PA Author Manuscript

NIH-PA Author Manuscript

NIH-PA Author Manuscript

cell permeability of drug candidates. Therefore, the ability to screen directly for potent RTK inhibitors in cells is highly sought after.

Furthermore, significant setbacks have been encountered with the current generation of approved inhibitors, resulting from rapid acquisition of resistance mutations in the kinase domain.[2] This observation highlights the need for identifying RTK inhibitors with an alternative mechanism of action, distinct from targeting the kinase activity of RTK. Interestingly, a strong link between endocytosis and signaling is emerging, with growing evidence revealing the key role of endocytosis in the compartmentalization of cell signaling components. While receptor endocytosis has long been known as a mechanism to attenuate ligand effect and to transport and recycle receptors, receptor trafficking is now increasingly seen as playing a direct role in triggering transduction signals.[3-6] Receptor signaling has been shown to continue in endosomal compartments following receptor activation; furthermore, certain signaling events have been demonstrated to require endocytosis.[5] Receptor trafficking can control the timing, amplitude, and specificity of signaling.[5] For this reason, the field would highly benefit from efficient methods to rapidly identify inhibitors of RTK activation and trafficking in cells.

Live cell-based assays have crucial advantages compared to in vitro assays relying on the use of purified recombinant proteins. Live cells recapitulate the endogenous environment surrounding RTKs, including their cell signaling networks with proteins expressed at physiological levels. In addition, because cell populations are heterogeneous in nature, assays measuring the overall response of the cell population in a well are prone to error. For this reason, high content assays are preferred, since they allow us to perform cell by cell analysis.[7] Therefore, cell based assays are necessary for the identification of cell-potent inhibitors of RTK activation, potentially targeting events distinct from tyrosine kinase phosphorylation.

We recently described the development of a novel cell based biosensor assay allowing the identification of EGFR modulators in high-throughput formats.[8] The assay relies in the expression, in A549 EGFR biosensor cells (A549-EGFRB cells), of a SRC Homology 2 domain (SH2) of GRB2 that specifically binds to activated EGFR, fused to Green Fluorescent Protein (GFP). Upon receptor activation following ligand stimulation, EGFR clustering, internalization and trafficking is visualized and granule formation imaged on the GFP channel is quantified as a surrogate for endogenous RTK activity in live cells (Fig 1). In addition, stained nuclei are imaged and quantified as a measure of cell number and cytotoxicity.

In this study, we sought to validate our domain-based biosensor assay for the identification of novel small molecule EGFR modulators by high throughput screening. We conducted a control run aimed at evaluating the robustness of the optimized EGFRB assay in the conditions used for automated screening, followed by a pilot screen of approximately 7,000 compounds tested in duplicate to assess the reproducibility and robustness of the assay; and its ability to identify inhibitors of EGFR activity in live cells. We confirmed the dose-dependent activity of obtained positives in the EGFRB assay and further assessed their activities in cell based viability assays as well as against an in vitro kinase panel. The results of this comprehensive study are described below.

## MATERIALS AND METHODS

### Materials

Reagents used for the EGFRB assay and for EGFR protein immunostaining and EGFR knockdown experiments were obtained as previously described.[9] A549 cells were purchased

NIH-PA Author Manuscript

NIH-PA Author Manuscript

NIH-PA Author Manuscript

from ATCC (catalogue #CCL-185). H2030, H3255 and HCC4011 Non Small Cell Lung Cancer Cells (NSCLC) were obtained from Dr. Romel Somwar (The Varmus Lab, MSKCC). DRAQ5 DNA dye was purchased from Biostatus (Leicestershire, UK). The "killer mix" used as a low control in viability assays consists of a proprietary mixture of cytotoxic compounds as previously described.[9-11] For the luminescence ADP production kinase assay, HEPES, ß-glycerol phosphate, $MgCl_2$, TCEP, Sodium orthovanadate, Poly(Glu,Tyr) peptide and Tween 80 were purchased from Sigma-Aldrich (Saint Louis, MO). ADP-Glo Kinase Assay Kit and ATP were purchased from Promega (Madison, WI). SRC, ABL and VEGFR1 kinase were purchased from Life Technologies (Grand Island, NY). EGFR kinase was purchased from Carna Biosciences (Kobe, Japan). Staurosporine was purchased from LC Laboratories (Woburn, MA).

## Assay control run

The performance of the EGFRB assay in the HTS conditions was assessed as previously described[8] in a control run consisting of three 384-well microtiter plates that contained 1% DMSO (v/v) for the high control and three 384-well microtiter plates that contained 10 μM gefitinib in 1% DMSO (v/v) for the low control. 5 μL of 10% DMSO (v/v) were added to the high control plates and 5 μL 100 μM gefitinib in 10% DMSO (v/v) were added to the low control plates with a custom designed 384 head on a PP-384-M Personal Pipettor (Apricot Designs, Monrovia, CA). A549-EGFRB cells were added to the plates in 45 μL cell culture media using an automated Multidrop 384 dispenser (Thermo Scientific, Waltham, MA) at the previously optimized cell density of 5,000 cells per well and incubated in Cytomat automated temperature- and humidity-controlled incubator (Thermo Scientific, Waltham, MA) at 37°C and 5% $CO_2$ for 16 hours. The cell culture media was then aspirated using an automated plate washer ELx405 (Biotek Instruments, WI) and replaced with media containing 500 nM Epidermal Growth Factor (EGF). Plates were further incubated in Cytomat for 70 minutes and cells were fixed following media aspiration using Biotek washer and dispensing of 50 μL 4% paraformaldehyde (v/v) in PBS using Multidrop. After 20 minutes incubation at room temperature and one wash with PBS using Multidrop and Biotek washer, cell nuclei were stained with 50 μl 2.5 μM DRAQ5 in PBS added using Multidrop. After 15 minutes incubation at room temperature, cells were washed twice with 50 μl PBS using Multidrop and Biotek Washer.

## Pilot screen

A pilot screen against the chemical library of 6,912 compounds described above was performed in duplicate according to the assay workflow described for the assay control run and at a screening concentration of 10 μM compound in 1% DMSO (v/v). Controls present in each assay plate consisted of 1% DMSO (v/v) (high control) and 10 μM gefitinib in 1% DMSO (v/v) (low control) final concentration. Plate fixing was automated on a linear track robotic platform (CRS F3 Robot System, Thermo Scientific, USA) with integrated Biotek washer and Multidrop for plate washing and liquid dispensing. For automated INCA2000 imaging, plate handling was conducted using the Orbitor RS Microplate Mover (Thermo Scientific, USA). Screening data files resulting from the automated image analysis described above with granule and nuclei count for each well were subsequently loaded onto the HTS Core Screening Data Management System, a custom built suite of modules for compound registration, plating and data management powered by ChemAxon Cheminformatic tools (ChemAxon, Hungary). The percentage inhibition in granule count and nuclei count was calculated for each compound based on control values present in each assay plate as follows.

The percentage inhibition in granule count was calculated based on both high and low control averages as follows:

NIH-PA Author Manuscript

NIH-PA Author Manuscript

NIH-PA Author Manuscript

$$\%\mathbf{I}_{\text{granule count}} = (\text{high control average} - \text{well value}) / (\text{high control average} - \text{low control average}) \times 100$$

The percentage inhibition in nuclei count was calculated as follows based only on high controls as low control nuclei count values are not lower than high control values:

$$\%\mathbf{I}_{\text{nuclei count}} = 100 - [(\text{well value}) / (\text{high control average}) \times 100]$$

### Assessment of the anti-proliferative effects of hits against a panel of established cell lines

The anti-proliferative effect of confirmed hits was assessed against a panel of established cell lines that includes those harboring wild type EGFR (A549-EGFRB, A549 and H2030 cell lines) and those harboring the activating L858R EGFR mutation (H3255 and HCC4011 cell lines). A549-EGFRB cells were cultured as previously described.[8] H2030, H3255 and HCC4011 cells were cultured as previously described.[12] A549 cells were cultured in F12K media (Invitrogen Cat.# 21127-022) supplemented with 10% FBS (PAA Cat.# A15-201). The anti-proliferative effect of each compound was assessed in dose response studies in 384-well format using 12 doubling dilutions in duplicate with 10 μM and 1 μM compound concentration as the upper limit and using the Alamar Blue viability assay as previously described.[13] Control wells consisted of 1% DMSO (v/v) (high control) and 1 μM "killer mix" in 1% DMSO (v/v) (low control). Final compound incubation time with cells was 120 hours. In dose response curves plotted using SigmaPlot 9.0 (Systat Software, San Jose, CA), the mean data from duplicates is presented and the error bars correspond to the standard error of the regression.

### Assessment of the inhibitory activity of hits against a panel of kinases

The activity of confirmed positives was assessed in a panel of kinases consisting of EGFR, VEGFR1, SRC and ABL kinase using a luminescence ADP production kinase assay as previously described.[14-16] The potency of each compound was measured in dose response studies in 384-well format using 12 doubling dilutions in duplicate with 10 μM and 1 μM compound concentration as the upper limit. All reagents transfers were performed using the PP-384-M Personal Pipettor. Tested compounds or controls were added to the wells at a volume of 1 μL to white 384 well microtiter plates (Corning #3570, Corning, NY). Controls consisted of 1% DMSO (v/v) (high control) and 30 μM staurosporine in 1% DMSO (v/v) (low controls). The assay buffer was 25 mM Hepes/NaOH, pH 7.5 and contained 10 mM $MgCl_2$, 2 mM TCEP, 20 mM β-Glycerol Phosphate, and 100 μM $Na_3VO_4$; for each kinase on the panel 4 μL of kinase dilution in assay buffer were added to the wells to reach a final concentration of 50 nM enzyme. Of note, the specific activity of the kinases of the panel is unknown and therefore the concentration of active enzyme in the preparation is unknown. After enzyme addition, kinase and compound were pre-incubated for 10 minutes at room temperature. Then 5 μL of a mix containing ATP and Poly(Glu, Tyr) substrates in solution in assay buffer were added to the wells both to reach a final concentration of 200 μM. After 45 minutes reaction at room temperature, 10 μL of ADP-Glo Reagent were added to each well. After 40 minutes incubation, 20 μL Kinase Detection Reagent were added followed by 60 minute incubation. The luminescence signal output was measured on the LEADseeker™. Dose response curves were plotted using SigmaPlot and represent the mean data from duplicates, the error bars correspond to the standard error of the regression. The low limit for calculating compound $IC_{50}$ in the assay conditions was 10 nM.

NIH-PA Author Manuscript

NIH-PA Author Manuscript

NIH-PA Author Manuscript

## RESULTS

We have previously established a proof of concept for a novel domain-based biosensor assay that allows us to screen for EGFR modulators in live cells.[8] Our goal in this study is to validate the optimized EGFRB assay for chemical screening and to assess whether it would allow for the identification of EGFR kinase modulators, to include activators and inhibitors, as well as those with an alternative mechanism of action.

### Assay control well assessment of the optimized EGFRB assay in HTS format

For this purpose, we first evaluated the robustness of the assay performed in the conditions of screening in a control run consisting of 1,152 high control wells containing 1% DMSO (v/v) and 1,152 low control wells containing 10 μM gefitinib in 1% DMSO (v/v). As expected, granule formation was triggered by stimulation with 500 nM EGF in the high control wells (Fig 2A1 & 4), while it was inhibited in the low control wells (Fig 2A2 & 5), mimicking the absence of EGF stimulation (Fig 2A3 & 6). Quantification of granule formation revealed a large signal window between high and low controls with an average granule count of 10,737 for high compared to 507 for low control wells (Figs 2B & 2C). This large signal window was accompanied with an acceptable variability for both the high and low controls, with a coefficient of variation (CV) of 13% and 14%, respectively. Combined with a signal to noise ratio of 21:1, this low variability translated into a calculated Z' value of 0.56, indicative of good assay performance and robustness (Fig 2C). As expected, nuclei count values were not significantly different between high and low controls, with an average imaged nuclei count of 1,219 for high controls compared to 1,200 for low controls and with CVs of 13% and 14%, respectively (Figs 2B & 2C). This result demonstrates that the observed difference in granule count between the two conditions is not due to a difference in cell number, rather the direct consequence of EGFR activity inhibition by gefitinib. Overall, the results from this control run demonstrate that the robustness of the EGFRB assay is compatible with HTS.

### Pilot screen against a library of 6,912 compounds

Following this positive result, we performed a pilot screen against a library of 6,912 FDA approved and known bioactive compounds in duplicate and at a compound screening concentration of 10 μM in 1% DMSO (v/v). We evaluated the reproducibility of the screen by plotting the granule count values induced by each compound and for each set of data as a scatter plot (Fig 3A). As expected, most compounds have no effect and cluster around a granule count value of 10,000 to 12,000, consistent with the average granule count for high controls of 10,737 observed in the assay control run; in contrast few compounds induced granule count values below 5,000. When plotting as a scatter plot the nuclei count values induced by each compound and for each set of data, most compounds had little effect on cell count with the cloud of compounds centered around a nuclei count of about 1,200 (Fig 3B), consistent with the average nuclei count value of 1,219 and 1,200 observed both for high and low controls respectively in the assay control run. This result is expected since most cytotoxic compound present in the library are not expected to be potent within the 17 hour timeframe of the assay, inferior to the doubling time of A549 cells. The linear shape of the cloud of compounds and the presence of few outliers for both the granule count and nuclei count scatter plots demonstrate the good reproducibility of our assay in the conditions of screening.

To assess whether EGFRB assay was able to identify EGFR inhibitors in live cells, we highlighted all described EGFR kinase inhibitors present in the library in the scatter plot of the average percentage inhibition in granule count for each compound against the average percentage inhibition it induced in nuclei count (Fig 3C). As an important result, 12 out of

NIH-PA Author Manuscript

NIH-PA Author Manuscript

NIH-PA Author Manuscript

13 reported EGFR kinase inhibitors are clustered in this scatter plot as inducing a high percentage inhibition in granule count and low percentage in nuclei count, as expected (Fig 3C, Table 1S). Erbstatin analog[17] with improved stability in serum compared to erbstatin was the only reported EGFR kinase inhibitors not identified as preventing granule formation in our assay and we included it in our follow up studies. Overall, our results strongly demonstrate the ability of our EGFRB assay to identify known EGFR kinase inhibitors using this novel screening approach.

Based on the performance of each compound in the granule count and nuclei count readout, we identified two populations of compounds: those compounds mimicking the performance of EGFR kinase inhibitors that inhibited granule count in absence of toxicity, as well as compounds that apparently induced an increase in granule formation in absence of an increase in cell count (Fig 3D). We selected 82 positives for inhibition of granule formation in our pilot screen as those compounds inducing greater than 60% inhibition of granule formation and less than 50% inhibition in nuclei count; resulting in an initial hit rate of 1.2 % (Table 1S). In addition, we selected 66 positives exhibiting activation of granule formation as those compounds inducing lower than -100% inhibition of granule formation and lower than 50% inhibition in nuclei count, and resulting in an initial hit rate of 0.95% (Table 2S). Of note, none of the selected activators induced any significant increase in nuclei count, indicating that the observed increase in granule count is not due to an increase in the number of cells (Table 2S). Out of the 148 identified and combined positives, we selected 27 inhibitors and 15 activators of granule formation to be resupplied for follow-up studies based on two pragmatic criteria: cost and availability of compounds (Tables 1S & 2S). Resupplied compounds included erbstatin analog and 8 other known EGFR kinase inhibitors. As part of our standard confirmatory workflow,[18] resupplied positives were tested for solubility and optical interference. One compound, in particular, was found to display significant auto-fluorescence interference in the GFP channel and was excluded from follow-up studies: the checkpoint kinase 1 inhibitor SB-218078 (Table 2S). When assessing compound solubility limit using laser nephelometry with 12 compound doubling dilutions and with 10 μM compound concentration as the upper limit, no compound was found to induce any significant dose-dependent increase in turbidity values, indicating that the solubility limit for all tested compounds was greater than 10 μM.

## Dose response studies of the confirmed EGFR inhibitors and activators

For confirmation of the identified positives in the EGFRB assay, we assessed the activity of the 42 resupplied positives in the EGFRB assay in dose response studies over 12 doubling dilutions from a high concentration of 10 μM compound. 13 of the 27 identified inhibitors of granule formation were confirmed as inhibitors in the EGFRB assay (48% confirmation rate) with a calculated $IC_{50}$ lower than 10 μM for inhibition of granule formation, along with a calculated $IC_{50}$ greater than 10 μM for nuclei count, indicating that the observed decrease in granule count is not due to a decrease in the number of cells. (Tables 1 & 3S). Of the 9 reported EGFR kinase inhibitors that were resupplied, 8 were confirmed in dose response; erbstatin analog, which we had not picked as positives, failed to induce any inhibition of granule formation in the EGFRB assay up to 10 μM, confirming our initial result during the screen (Table 1). Among the EGFR kinase inhibitors that confirmed their activity in the EGFRB assay were all 3 FDA-approved small molecule EGFR kinase inhibitors erlotinib ($IC_{50}$ = 0.21±0.03 μM), gefitinib ($IC_{50}$ = 0.38±0.04 μM) and lapatinib ($IC_{50}$ = 0.59±0.03 μM) (Table 1 &3S), demonstrating the ability of our assay to identify cell potent EGFR kinase inhibitors. Among described EGFR kinase inhibitors, $IC_{50}$s ranged from the most potent compound BIBU 1361 ($IC_{50}$ =0.038±0.007 μM) to the least potent compound erbstatin analog ($IC_{50}$ > 10 μM); and we included erbstatin analog inactive in our assay for follow up studies with a panel of kinases. The trend in potency observed in the

NIH-PA Author Manuscript

NIH-PA Author Manuscript

NIH-PA Author Manuscript

EGFRB assay generally matched reported activities toward recombinant EGFR kinase for these compounds: from the potent BIBU 1361 EGFR kinase inhibitor ($IC_{50}$ = 0.003 μM)[19] to the weak PKC412 EGFR kinase inhibitor ($IC_{50}$ = 3.0 μM).[20] This observation highlights the high relevance of our assay for the identification of cell permeable EGFR kinase inhibitors. Interestingly, among the confirmed inhibitors of granule formation was the VEGFR (Flt and KDR) kinase inhibitor ZM-306416[21] ($IC_{50}$ = 0.67±0.2 μM) (Fig 1AS), not described as potent toward EGFR kinase in the literature but sharing the 4-anilinoquinazoline scaffold common among EGFR kinase inhibitors such as erlotinib, gefitinib and lapatinib (Table 3S). This result demonstrates the ability of our assay to identify novel EGFR kinase inhibitors with potent cellular activities. Importantly, among the confirmed inhibitors was the Hsp90 inhibitor 17-DMAG;[22] this result is not surprising since Hsp90 inhibition is known to suppress EGFR signaling[23], as EGFR is a client protein of Hsp90, however it demonstrates the ability of our assay to identify inhibitors of EGFR activation distinct from inhibitors of EGFR kinase inhibitors.

Among the 15 resupplied activators of granule formation, 3 were confirmed as activators in the EGFRB assay (20% confirmation rate) with a calculated $EC_{50}$ lower than 10 μM for activation of granule formation, along with a calculated $EC_{50}$ greater than 10 μM for nuclei count. As a control, granules were not observed when we imaged A549 parental cells in the GFP channel after treatment with the identified activators of granule formation, ruling out the possibility that the observed increase in granules results from an artifact. The 3 confirmed activators were the steroids flurandrenolide ($EC_{50}$ = 0.023±0.02 μM) (Fig 1BS) and beclomethasone ($EC_{50}$ = 0.042±0.007 μM); and the H1 receptor antagonist ebastine ($EC_{50}$ = 1.5±0.3 μM) (Tables 1 & 3S). Importantly, nuclei count upon treatment with the confirmed activators up to 10 μM did not increase significantly, indicating that the observed increase in granule count is not due to an increase in the cell number, but rather corresponds to an increase in granule count per cell induced by these compounds through an unknown mechanism.

## Cytotoxicity assessment of the confirmed EGFR inhibitors and activators

To further characterize the activity of the confirmed positives in the EGFRB assay, we assessed the dose response in the Alamar Blue viability assay of confirmed granule formation inhibitors and activators toward wild type EGFR cells (A549-EGFRB, A549 and H2030 cells), as well as the EGFR addicted H3255 and HCC4011 human NSCLC cells harboring the activating L858R EGFR mutation. Not surprisingly, all known EGFR inhibitors that confirmed in our assay had potent cytotoxic activity toward the H3255 and HCC4011 cell lines such as gefitinib with an $IC_{50}$ of respectively < 0.01 μM and 0.028±0.003 μM toward H3255 and HCC4011 cells respectively, while having no or low effect toward the wild type EGFR cell lines A549 and H2030 ($IC_{50}$ > 10 μM) (Fig 4, Table 2). An important result was that the reported EGFR kinase inhibitor erbstatin analog did not have any significant anti-proliferative effect toward any of the cell lines tested, inducing only partial inhibition in the Alamar Blue viability assay up to 10 μM (Fig 4, Table 2). This result is in agreement with our previous findings according to which erbstatin analog exhibited no activity in the EGFRB assay. Confirming the newly identified inhibitory activity of ZM-306416 toward EGFR, this compound induced selective anti-proliferative effect toward the EGFR addicted NSCLC cell lines H3255 and HCC4011 ($IC_{50}$ = 0.09±0.007 μM and 0.072±0.001 μM respectively), while sparing the wild type EGFR cell lines A549 and H2030 ($IC_{50}$ > 10 μM) (Fig 4).

Of note, none of the confirmed granule activators induced any significant effect toward the viability of our cell panel (Table 2). This is an expected result, since these compounds did not significantly affect the nuclei count during the screen (Table 2S) and therefore are not expected to be toxic to the wild type EGFR cells A549 and H2030. In addition, since the

NIH-PA Author Manuscript

NIH-PA Author Manuscript

NIH-PA Author Manuscript

increase in granule count induced by these compounds is indicative of a stimulation of EGFR activation rather than its inhibition, the confirmed activators are not expected to prevent the proliferation of the mutant EGFR cells H3255 and HCC4011. Altogether, our results validate our strategy, in that we have successfully developed a novel assay able to identify drug candidates targeting EGFR activation in live cells.

### Kinase activity assessment of the confirmed hits against a panel of four kinases

We further characterized confirmed positives by assessing their potency in a luminescence ADP production kinase toward a panel of kinases assay that included EGFR, VEGFR1, ABL and SRC kinase. As expected, the 8 resupplied known EGFR kinase inhibitors inhibited EGFR kinase activity with $IC_{50}$ values consistently in the nanomolar range (Table 3). Interestingly, the described EGFR kinase erbstatin analog was inactive against all kinases tested, including its target EGFR. This result confirms our observation that this compound was inactive in the EGFRB assay and had no observed cytotoxicity effects on the H3255 and HCC4011 cell lines harboring the activating L858R EGFR mutation. ZM-306416 was found to be very potent toward the EGFR kinase with an $IC_{50}$ value lower than 10 nM, reaching our assay detection limit and confirming our result using the EGFRB assay (see above). ZM-306416 exhibited inhibitory activity across all three kinases of the panel, yielding $IC_{50}$ values of 0.33±0.08 μM for SRC, 0.33±0.04 μM for VEGFR1, and 1.3±0.2 μM for ABL kinases (Fig 5 & Table 3). While the other confirmed inhibitors of granule formation distinct from described EGFR kinase inhibitors have a calculated $IC_{50}$ toward EGFR kinase greater than 10 μM, it is important to note that they do induce partial inhibition of EGFR kinase activity, which could potentially explain their potency in the EGFRB assay. Partial inhibition of nuclei count induced by these compounds could also contribute to the observed decrease in granule count (Table 1).

Of note, the 3 confirmed activators of granule formation, flurandrenolide, beclomethasone and ebastine, have no inhibitory effects on the enzymatic activity of the kinases on the panel (**Table 3**). This is an expected result, since the increase in granule count induced by these compounds is indicative of a stimulation of EGFR activation rather than its inhibition, and to our knowledge those compounds have no reported inhibitory activity toward kinases.

## DISCUSSION

Targeting RTKs has proven to constitute a successful strategy for the development of novel antitumor agents potent in the clinic. As an example, there are currently 3 small molecule drugs approved by the FDA that target EGFR: gefitinib (Iressa), erlotinib (Tarceva) and lapatinib (Tykerb, Tyverb). All three drugs are 4-anilinoquinazoline based chemicals and share the same inhibitory mechanism of action (Table 3S); they target the tyrosine kinase activity of EGFR by competing for ATP binding. This common mechanism is believed to constitute a major limitation of current drugs targeting EGFR and other RTKs; where acquired resistance eventually develops in patients due to escape mutations appearing in the kinase domain and in some cases in the ATP binding pocket of the enzyme. [2]

Current drugs eventually become inactive in those patients developing mutations, and as such there is a need to rapidly identify new drug candidates overcoming resistance. However, current approaches to identify new drug candidates targeting RTKs are rather slow with a high attrition rate of leads, hampering the discovery of novel candidates. The failure of many lead candidates during development is due to the fact that they are identified in HTS screens relying on assays measuring the kinase activity of recombinant kinases. Very often, potent molecules in vitro fail the transition to being potent when tested in cellular assays, since such assays are highly artificial compared to physiological protein expression levels, together with the complexity of the cellular environment and the presence

NIH-PA Author Manuscript

NIH-PA Author Manuscript

NIH-PA Author Manuscript

of interconnected signaling pathways. The current low success rate of drug candidates targeting RTKs can therefore be attributed to the lack of cell based assays that would allow direct identification of RTK inhibitors. In addition, since currently available assays amenable to high throughput screening all measure the kinase activity of the receptor, all drug candidates discovered through this process share the same limitations of kinase inhibitors in regards to the appearance of resistance in patients.

For this reason, we sought to explore the use of domain-based biosensors of RTK activation, and after developing a domain-based EGFR biosensor as a proof of concept,[8] we aimed at validating this new technology for high throughput screening (Fig 1). In this article, we show that our miniaturized assay in 384-well format is robust, with a Z' of 0.56 in a control run performed in the conditions of screening (Figs 2B & 2C). In addition, scatter plot representation of the performance of each compound tested in duplicate in our screen of 6,912 bioactive compounds is indicative of the good reproducibility of our assay (Figs 3A & 3B). For positive compounds present in the library as multiple instances provided by different suppliers, the observation that we picked as positives several of each instance of those compounds further demonstrates the good reproducibility of the EGFRB assay in the conditions of screening, as this was the case for example with tyrphostin AG 1478, PD 153035, camptothecin, cycloheximide, lycorine and emetine for the identified inhibitors of granule formation (Table 1S), and flurandrenolide, beclomethasone and several other corticosteroids for the identified activators of granule formation (Table 2S). For those confirmed inhibitors of granule formation that were present in the library as provided by more than one supplier, tyrphostin AG 1478 and PD 153035 were in duplicate in the screened library and both instances were picked as positives. Erbstatin analog was also present in duplicate, and neither of its instances was potent in the screen, in agreement with our observation that erbstatin analog does not inhibit EGFR kinase. Altogether, our results demonstrate that our optimized EGFRB assay is robust and reproducible under HTS conditions, and further validating its use for screening larger chemical libraries.

Our results validated our approach, in that we have developed an assay that allowed the identification of 12 out 13 reported EGFR kinase inhibitors present in the screened library, including the 3 FDA approved EGFR kinase inhibitors gefitinib, erlotinib and lapatinib (Tables 1 & 3S). This is an important result, since to our knowledge, this study constitutes the first report of a method allowing the identification of EGFR kinase inhibitors directly in live cells. Of note, erbstatin analog, which was the only reported EGFR kinase that we failed to identify as a positive during screening (Fig 3C, Table 1), failed to inhibit the EGFR kinase activity in a previously validated luminescence ADP production assay (Fig 5), confirming the current results. All the other described EGFR kinase inhibitors present in the library were identified as positives in the screen (Table 1), and confirmed in dose response studies using the EGFRB assay (Table 1). They were subsequently found to be selectively potent cytotoxic agents towards the H3255 and HCC4011 cell lines harboring the activating L858R EGFR mutation (Table 2); and inhibited in-vitro EGFR kinase activity (Table 3). Taken together, these results clearly demonstrate that our novel approach enables the identification of cell permeable and potent EGFR inhibitors in live cells.

In addition, we have discovered that the VEGFR (Flt and KDR) kinase inhibitor ZM-306416[21], a previously not described inhibitor of EGFR as an inhibitor of granule formation in the EGFRB assay (Fig 1AS). Follow up studies confirmed ZM-306416 as a potent inhibitor of the EGFR in vitro kinase activity with an $IC_{50}$ value below 10 nM, the detection limit of the assay (Fig 5, Table 3). ZM-306416 was also found to inhibit the ABL in vitro kinase activity with a less potent $IC_{50}$ value of 1.3±0.2 μM toward the ABL kinase (Table 3). Furthermore, ZM-306416, as well as all of the other confirmed EGFR inhibitors in the granule formation assay were selectively potent toward cell lines harboring the L858R

NIH-PA Author Manuscript

NIH-PA Author Manuscript

NIH-PA Author Manuscript

EGFR mutation (H3255 and HCC4011 cell lines) as compared to those expressing wild type EGFR (A549 cell line) and mutated KRAS (H2030 cell line) (Fig 4), confirming that the inhibitors of granule formation that we identified target EGFR activity in the EGFRB assay. Therefore, our results demonstrate that this approach allows for the identification of known as well as novel cell permeable and potent EGFR inhibitors such as the VEGFR kinase inhibitor ZM-306416.[21]

Besides the known EGFR inhibitors and the discovery of ZM-306416 as an EGFR inhibitor, several confirmed hits with distinct biological activities were also identified in the pilot screen. Among them were camptothecin, a topoisomerase I inhibitor and potent cytotoxic agent[24], PKC412, a pan active kinase inhibitor reported to exhibit weak activity against EGFR ($IC_{50}$ = 3.0 μM)[20], aminopurvalanol A, an inhibitor of various CDKs[25], and 17-DMAG, an HSP90 inhibitor and potent cyotoxic agent[22]. Camptothecin, PKC412 and aminopurvalanol A were not found to be potent toward EGFR kinase, or induced only partial inhibition of EGFR kinase activity up to 10 μM (Table 3); those 3 compounds also induced partial inhibition of EGFRB cells nuclei count (Table 1), indicating that the observed reduction in granule count in the EGFRB assay may result from a combination of partial inhibition of kinase activity and cell count. 17-DMAG, however, induced potent inhibition of granule formation ($IC_{50}$ = 0.029±0.003 μM) in absence of any effect on nuclei count (Table 1 & 3S). This is an interesting and expected result since EGFR is a client protein of Hsp90 and inhibiting EGFR maturation will de facto prevent its activation.[23] Not surprisingly, we also selected as inhibitors of granule formation 3 other described HSP90 inhibitors: geldanamycin, 17-AAG and CCT 018159 (Table 1S). Of note, CCT 018159 was resupplied and not selected as a confirmed inhibitor with a calculated $IC_{50}$ lower than 10 μM (Table 1S); however partial inhibition was observed at 5 and 10 μM, confirming our initial observation during the screen. The identification of HSP90 inhibitors as inhibitors of granule formation in our assay emphasizes a major advantage of screening for RTK inhibitors directly in cells, as this opens the door to identify modulators of all steps of RTK activation, such as maturation, dimerization, and trafficking. Such inhibitors are highly sought, as they would constitute an alternative to inhibitors of the kinase domain of RTK, which use is severely limited due to appearance of resistance in patients. Since receptor trafficking controls the timing, amplitude, and specificity of signaling,[5] targeting the interface between the trafficking of a specific receptor and the signaling events it triggers constitutes an attractive alternative to inhibiting RTK kinase activity for the discovery of potent new anticancer drugs that overcome acquired resistance to current treatment. In summary, our results highlight the power of our approach, in that we could identify EGFR inhibitors distinct from EGFR kinase inhibitors.

In addition, our results demonstrate the versatility of our approach, in that we have unexpectedly identified confirmed activators of granule formation such as flurandrenolide (Fig 1BS, Tables 1 & 3S). Two confirmed activators of granule formation (flurandrenolide and beclomethasone) belong to the class of corticosteroids and interestingly, 30 out of the 66 activators identified in the screen belong to the same class (Table 2S). While their mechanism of action is currently unclear, these new chemical probes may reveal novel mechanism of EGFR regulation. This important finding illustrates the power of screening for modulators of a given target in live cells, as it can yield unexpected fundamental discoveries.

In conclusion, we anticipate that our approach allows us to accelerate the discovery of potent drugs targeting RTKs. The ability to screen for modulators of mutated endogenous RTK in cells derived from patients opens the door to the rapid identification of drug candidates overcoming the specific mechanism of resistance developed in each patient. Furthermore, assays relying on domain-based biosensor can easily be adapted to conducting RNAi

NIH-PA Author Manuscript

NIH-PA Author Manuscript

NIH-PA Author Manuscript

screening, allowing the identification of genes involved in signaling pathways in relation to the RTK of interest. For these reasons, we expect that the validated domain-based biosensor technology that we describe in this manuscript will accelerate drug discovery as well the understanding of complex signaling pathways related to RTKs.

## Supplementary Material

Refer to Web version on PubMed Central for supplementary material.

## Acknowledgments

The authors would like to thank Constantin Radu, Alun Bermingham and members of the HTS Core Facility for their help during the course of this study, and our colleagues Dmitry Malkov, Keming Song and John Fetter at Sigma-Aldrich. The authors also thank Tony Riley and Terry Helms for their help with the artwork in this manuscript. The HTS Core Facility is partially supported by Mr. William H. Goodwin and Mrs. Alice Goodwin and the Commonwealth Foundation for Cancer Research, the Experimental Therapeutics Center of MSKCC, the William Randolph Hearst Fund in Experimental Therapeutics, the Lillian S. Wells Foundation, and by a NIH/NCI Cancer Center Support Grant 5 P30 CA008748-44.

## REFERENCES

1. Gschwind A, Fischer OM, Ullrich A. The discovery of receptor tyrosine kinases: targets for cancer therapy. Nat. Rev. Cancer. 2004; 4:361–370. [PubMed: 15122207]
2. Pao W, Chmielecki J. Rational, biologically based treatment of EGFR-mutant non-small-cell lung cancer. Nat. Rev. Cancer. 2010; 10:760–774. [PubMed: 20966921]
3. Clague MJ, Urbe S. The interface of receptor trafficking and signalling. J. Cell. Sci. 2001; 114:3075–3081. [PubMed: 11590234]
4. Platta HW, Stenmark H. Endocytosis and signaling. Curr Opin Cell Biol. 2011; 23:393–403. [PubMed: 21474295]
5. Sadowski L, Pilecka I, Miaczynska M. Signaling from endosomes: location makes a difference. Exp. Cell. Res. 2009; 315:1601–1609. [PubMed: 18930045]
6. Shilo BZ, Schejter ED. Regulation of developmental intercellular signalling by intracellular trafficking. EMBO J. 2011; 30:3516–3526. [PubMed: 21878993]
7. Ramirez CN, Antczak C, Djaballah H. Cell viability assessment: toward content-rich platforms. Expert Opinion on Drug Discovery. 2010; 5:223–233. [PubMed: 22823019]
8. Antczak C, Bermingham A, Calder P, Malkov D, Song K, Fetter J, Djaballah H. Domain-based Biosensor Assay to Screen for Epidermal Growth Factor Receptor Modulators of Live Cells. Assay Drug Dev. Technol. 2012; 10:24–36. [PubMed: 22280060]
9. Ibanez G, Shum D, Blum G, Bhinder B, Radu C, Antczak C, Luo M, Djaballah H. A High Throughput Scintillation Proximity Imaging Assay for Protein Methyltransferases. Comb Chem. High Throughput Screen. Jan 17.2012 [Epub ahead of print].
10. Antczak C, Kloepping C, Radu C, Genski T, Muller-Kuhrt L, Siems K, de Stanchina E, Abramson DH, Djaballah H. Revisiting old drugs as novel agents for retinoblastoma: in vitro and in vivo antitumor activity of cardenolides. Invest. Ophthalmol. Vis. Sci. 2009; 50:3065–3073. [PubMed: 19151399]
11. Tseng HM, Shum D, Bhinder B, Escobar S, Veomett NJ, Tomkinson AE, Gin DY, Djaballah H, Scheinberg DA. A High-Throughput Scintillation Proximity-Based Assay for Human DNA Ligase IV. Assay Drug Dev. Technol. Dec 22.2011 [Epub ahead of print].
12. Somwar R, Erdjument-Bromage H, Larsson E, Shum D, Lockwood WW, Yang G, Sander C, Ouerfelli O, Tempst PJ, Djaballah H, Varmus HE. Superoxide dismutase 1 (SOD1) is a target for a small molecule identified in a screen for inhibitors of the growth of lung adenocarcinoma cell lines. Proc. Natl. Acad. Sci. U S A. 2011; 108:16375–16380. [PubMed: 21930909]
13. Shum D, Radu C, Kim E, Cajuste M, Shao Y, Seshan VE, Djaballah H. A high density assay format for the detection of novel cytotoxic agents in large chemical libraries. J Enzyme Inhib. Med. Chem. 2008; 23:931–945. [PubMed: 18608772]

NIH-PA Author Manuscript

NIH-PA Author Manuscript

NIH-PA Author Manuscript


14. Takagi T, Shum D, Parisi M, Santos RE, Radu C, Calder P, Rizvi Z, Frattini MG, Djaballah H. Comparison of luminescence ADP production assay and radiometric scintillation proximity assay for Cdc7 kinase. Comb. Chem. High Throughput Screen. 2011; 14:669–687. [PubMed: 21564015]
15. Tanega C, Shen M, Mott BT, Thomas CJ, MacArthur R, Inglese J, Auld DS. Comparison of bioluminescent kinase assays using substrate depletion and product formation. Assay Drug Dev. Technol. 2009; 7:606–614. [PubMed: 20059377]
16. Zegzouti H, Zdanovskaia M, Hsiao K, Goueli SA. ADP-Glo: A Bioluminescent and homogeneous ADP monitoring assay for kinases. Assay Drug Dev. Technol. 2009; 7:560–572. [PubMed: 20105026]
17. Umezawa K, Hori T, Tajima H, Imoto M, Isshiki K, Takeuchi T. Inhibition of epidermal growth factor-induced DNA synthesis by tyrosine kinase inhibitors. FEBS Lett. 1990; 260:198–200. [PubMed: 2298299]
18. Antczak C, Shum D, Escobar S, Bassit B, Kim E, Seshan VE, Wu N, Yang G, Ouerfelli O, Li YM, Scheinberg DA, Djaballah H. High-throughput identification of inhibitors of human mitochondrial peptide deformylase. J. Biomol. Screen. 2007; 12:521–535. [PubMed: 17435169]
19. Solca FF, Baum A, Langkopf E, Dahmann G, Heider KH, Himmelsbach F, van Meel JC. Inhibition of epidermal growth factor receptor activity by two pyrimidopyrimidine derivatives. J. Pharmacol. Exp. Ther. 2004; 311:502–509. [PubMed: 15199094]
20. Meyer T, Regenass U, Fabbro D, Alteri E, Rosel J, Muller M, Caravatti G, Matter A. A derivative of staurosporine (CGP 41 251) shows selectivity for protein kinase C inhibition and in vitro anti-proliferative as well as in vivo anti-tumor activity. Int. J. Cancer. 1989; 43:851–856. [PubMed: 2714889]
21. Hennequin LF, Thomas AP, Johnstone C, Stokes ES, Ple PA, Lohmann JJ, Ogilvie DJ, Dukes M, Wedge SR, Curwen JO, Kendrew J, Lambert-van der Brempt C. Design and structure-activity relationship of a new class of potent VEGF receptor tyrosine kinase inhibitors. J. Med. Chem. 1999; 42:5369–5389. [PubMed: 10639280]
22. Smith V, Sausville EA, Camalier RF, Fiebig HH, Burger AM. Comparison of 17-dimethylaminoethylamino-17-demethoxy-geldanamycin (17DMAG) and 17-allylamino-17-demethoxygeldanamycin (17AAG) in vitro: effects on Hsp90 and client proteins in melanoma models. Cancer Chemother. Pharmacol. 2005; 56:126–137. [PubMed: 15841378]
23. Sawai A, Chandarlapaty S, Greulich H, Gonen M, Ye Q, Arteaga CL, Sellers W, Rosen N, Solit DB. Inhibition of Hsp90 down-regulates mutant epidermal growth factor receptor (EGFR) expression and sensitizes EGFR mutant tumors to paclitaxel. Cancer Res. 2008; 68:589–596. [PubMed: 18199556]
24. Ulukan H, Swaan PW. Camptothecins: a review of their chemotherapeutic potential. Drugs. 2002; 62:2039–2057. [PubMed: 12269849]
25. Chang YT, Gray NS, Rosania GR, Sutherlin DP, Kwon S, Norman TC, Sarohia R, Leost M, Meijer L, Schultz PG. Synthesis and application of functionally diverse 2,6,9-trisubstituted purine libraries as CDK inhibitors. Chem. Biol. 1999; 6:361–375. [PubMed: 10375538]

NIH-PA Author Manuscript

NIH-PA Author Manuscript

NIH-PA Author Manuscript

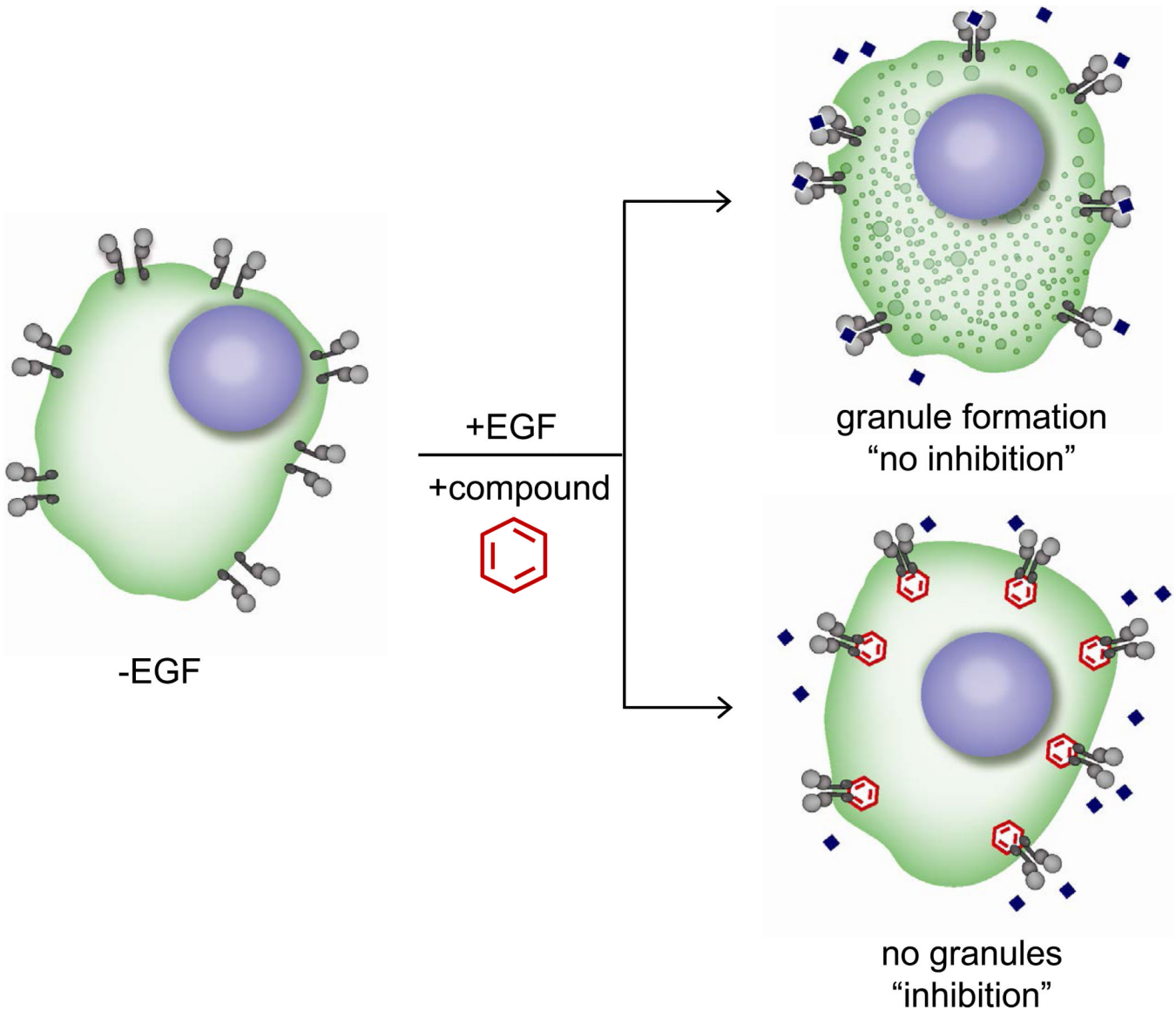


**Figure 1. Principles of the EGFRB assay**

Schematics of the EGFRB assay with A549 EGFR biosensor cell line (A549-EGFRB). In absence of EGF stimulation, diffused GFP is observed in the cytoplasm of cells. In contrast, EGF addition triggers EGFR activation and subsequent clustering and internalization as observed by the formation of granules (vesicles) in the GFP channel, corresponding to “no inhibition”. Granule formation upon EGF stimulation is prevented by EGFR small molecule inhibitors (“inhibition”), allowing the identification of novel EGFR inhibitors by HTS.

NIH-PA Author Manuscript

NIH-PA Author Manuscript

NIH-PA Author Manuscript

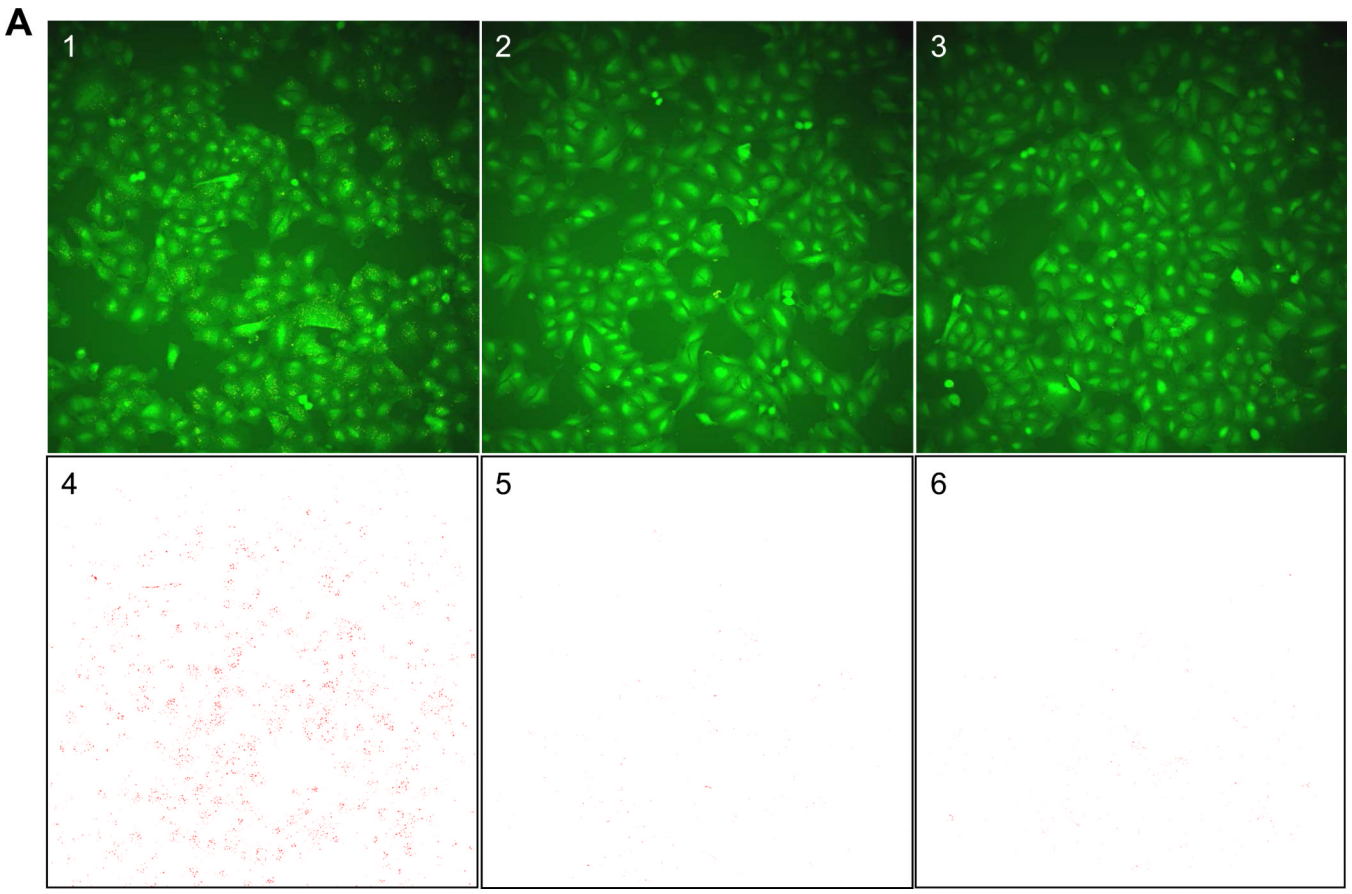

NIH-PA Author Manuscript

NIH-PA Author Manuscript

NIH-PA Author Manuscript

B

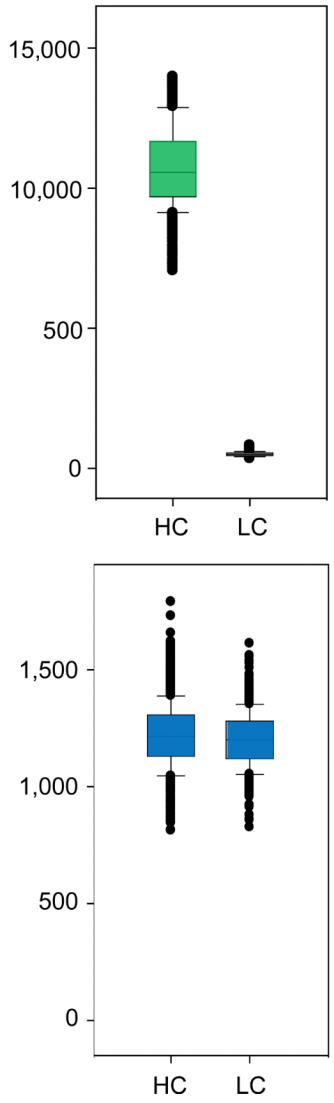


C

| granule count | average count | std. deviation | CV | S/N | Z' |
|---|---|---|---|---|---|
| HC | 10,737 | 1,412 | 13% | 21 | 0.56 |
| LC | 507 | 73 | 14% | | |

| nuclei count | average count | std. deviation | CV |
|---|---|---|---|
| HC | 1,219 | 138 | 11% |
| LC | 1,200 | 114 | 9% |

**Figure 2. Control well images and control run assessment of the EGFRB assay**

**A)** INCA2000 images of A549-EGFRB cells in control wells in 384-well microtiter plate format. **1)** Granules are observed specifically upon stimulation with 500 nM EGF in control wells containing 1% DMSO (v/v). **2)** In control wells containing 10 μM gefitinib in 1%DMSO (v/v), granule formation is prevented even in the presence of 500 nM EGF. **3)** Assay well in the absence of EGF stimulation show lack of granule formation. The overlay of automated granule segmentation is represented in red for **4)** control wells containing 1% DMSO (v/v), **5)** control wells containing 10 μM gefitinib in 1%DMSO (v/v) and **6)** assay wells in absence of EGF stimulation. Control wells in the EGFRB assay control run, pilot screen and subsequent dose response studies consist of high control wells (1%DMSO (v/v) final) (**1**) and low control wells (10 μM gefitinib in 1%DMSO (v/v)) in presence of 500 nM EGF stimulation (**2**). **B)** Scatter plot analysis of high control (HC) and low control (LC) wells for the EGFRB assay control run in the granule count and nuclei count readout. **C)** Summary table of statistics for the EGFRB assay control run. The average granule count and nuclei count, standard deviation, coefficient of variation (CV) for high and low controls, signal to noise ratio (S/N), and calculated Z' value are presented.

NIH-PA Author Manuscript
NIH-PA Author Manuscript
NIH-PA Author Manuscript



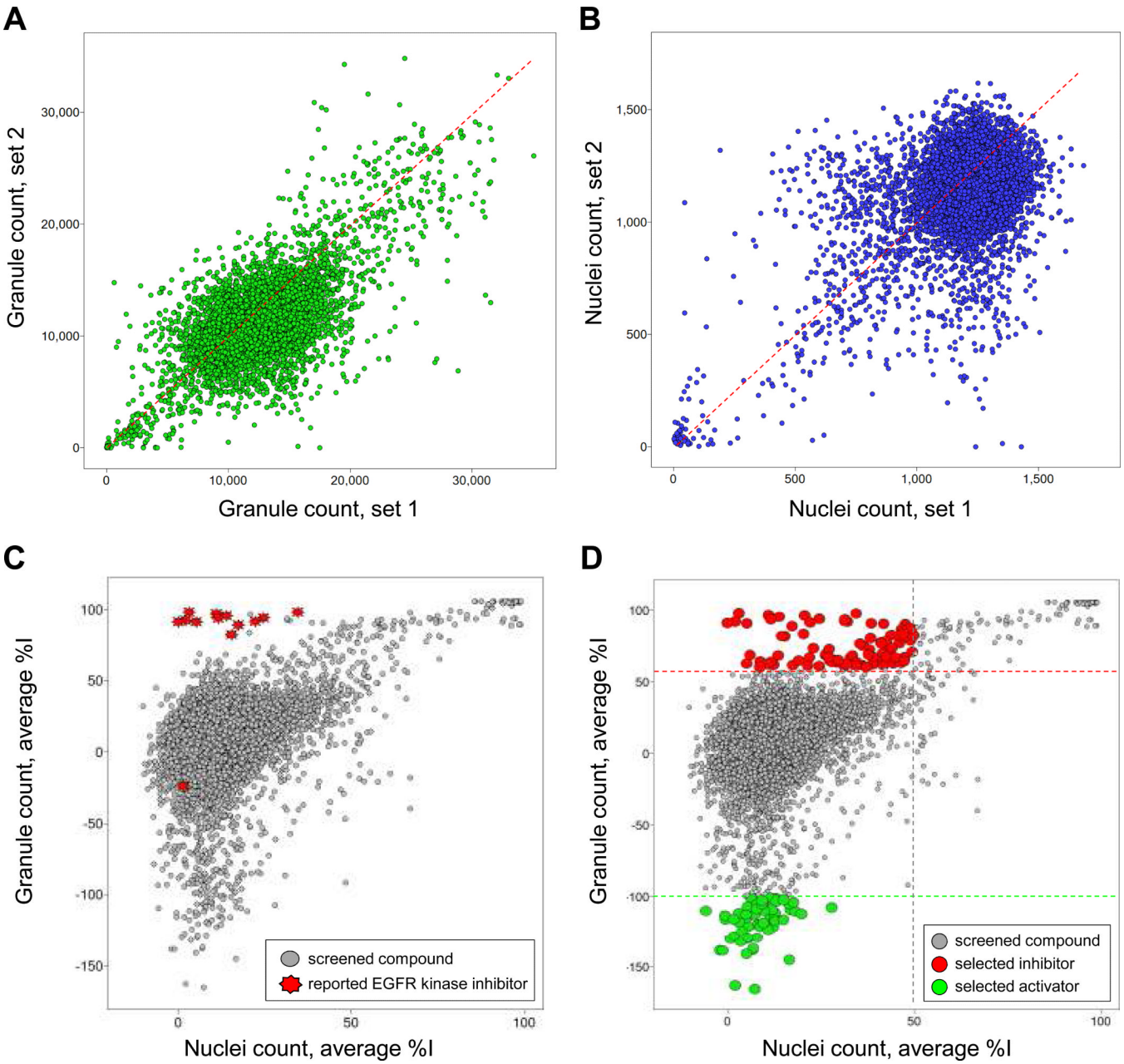


**Figure 3. Scatter plot analysis of the pilot screen performed in duplicate**

A library of 6,912 compounds was screened in duplicate to evaluate assay reproducibility and performance. **A)** The granule count for each compound and for each set of data is plotted as a scatter plot, demonstrating the reproducibility of the granule count readout during the pilot screen. **B)** The nuclei count for each compound and for each set of data is plotted as a scatter plot, demonstrating the reproducibility of the nuclei count readout during the pilot screen. **C)** and **D)** The average percentage inhibition in granule count for each compound for both replicate sets of data is plotted against the average percentage inhibition in nuclei count of each compound for positive selection. **C)** 12 out of 13 reported EGFR kinase inhibitors are clustered in the scatter plot inducing a high percentage inhibition in granule count and low percentage in nuclei count. **D)** Positives for inhibition of granule formation in the pilot screen are selected as those compounds inducing greater than 60%

inhibition of granule formation and less than 50% inhibition in nuclei count. Activators of granule formation in the pilot screen are selected as those compounds inducing lower than -100% inhibition of granule formation an lower than 50% inhibition in nuclei count.

NIH-PA Author Manuscript
NIH-PA Author Manuscript
NIH-PA Author Manuscript

NIH-PA Author Manuscript
NIH-PA Author Manuscript
NIH-PA Author Manuscript



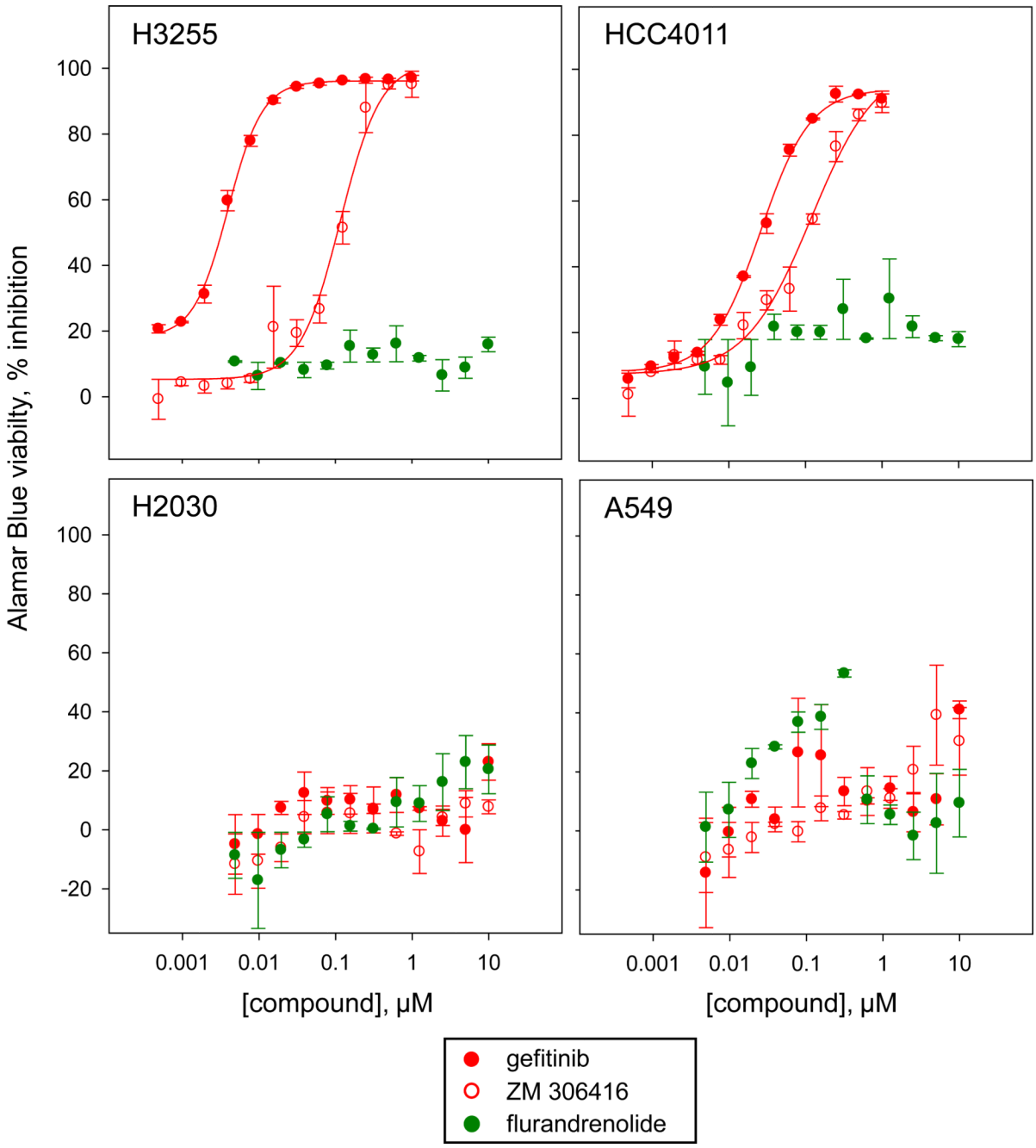


**Figure 4. Assessment of the selective anti-proliferative effect of confirmed positives toward EGFR mutant cell lines**

Dose response studies of the compounds gefitinib, ZM-306416 and flurandrenolide in the Alamar Blue viability assay against the H3255 and the HCC4011 cell lines harboring the activating EGFR mutation L858R as compared to the wild type EGFR cell lines H2030 and A549. The EGFR kinase inhibitor gefitinib is selectively potent toward the EGFR mutant H3255 and HCC4011 cells, with a calculated $IC_{50}$ of < 0.01 μM and 0.028±0.003 μM respectively. Similarly, ZM-306416 is selectively potent toward the EGFR mutant H3255 and HCC4011 cells, with a calculated $IC_{50}$ of 0.09±0.007 μM and 0.072±0.01 μM, respectively. Both gefitinib and ZM-306416 are inactive toward the wild type EGFR cell

lines H2030 and A549. The confirmed activator of granule formation flurandrenolide is inactive toward both the EGFR mutant and wild type cell lines tested.

NIH-PA Author Manuscript
NIH-PA Author Manuscript
NIH-PA Author Manuscript

NIH-PA Author Manuscript
NIH-PA Author Manuscript
NIH-PA Author Manuscript



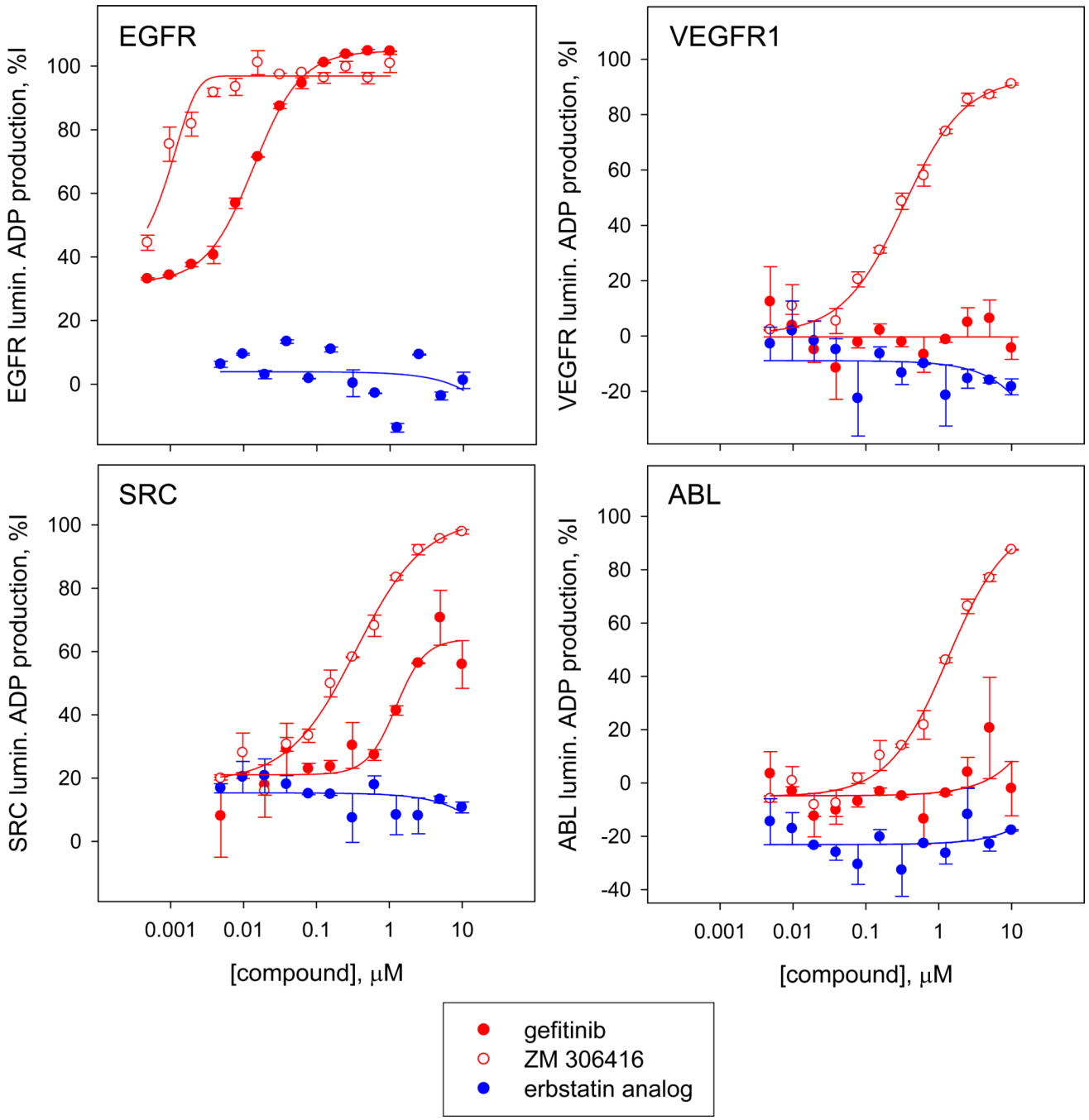


**Figure 5. Assessment of potency of selected hits in a panel of kinases using the luminescence ADP production kinase assay**

Dose response studies of gefitinib, ZM-306416 and the erbstatin analog against a kinase panel consisting of the kinases EGFR, VEGFR1, SRC and ABL. The EGFR kinase inhibitor gefitinib is selectively potent toward EGFR, with a calculated $IC_{50}$ of < 0.01 μM, and low or no activity toward VEGFR1 ($IC_{50}$ > 10 μM), SRC ($IC_{50}$ > 10 μM) and ABL ($IC_{50}$ > 10 μM). In contrast, ZM-306416 is potent toward all kinases of the panel: EGFR ($IC_{50}$ < 0.01 μM), VEGFR1 ($IC_{50}$ = 0.33±0.04 μM), SRC ($IC_{50}$ = 0.33±0.08 μM) and ABL ($IC_{50}$ =1.3±0.2 μM). Erbstatin analog is inactive ($IC_{50}$ > 10 μM) toward all kinases in the panel, including EGFR kinase.

NIH-PA Author Manuscript NIH-PA Author Manuscript NIH-PA Author Manuscript



**Table 1**

**Performance of 16 hits and erbstatin analog in the EGFRB assay**

The average percentage inhibition at 10 μM compound concentration during the screen and the $IC_{50}$ or $EC_{50}$ values ±standard deviation calculated based on follow up dose response studies are summarized for both the granule count and nuclei count readouts.

| | | | HTS % inhibition at 10 μM | | $IC_{50}$ or $EC_{50}$ (nM) | |
|---|---|---|---|---|---|---|
| | **Compound name** | **Molecular target** | **Granule count** | **Nuclei count** | **Granule count** | **Nuclei count** |
| Known EGFR inhibitors | BIBU 1361 | EGFR kinase | 98 | 3 | 38±7 | N.E. |
| | Tyrphostin AG 1478 | EGFR kinase | 94 | 12 | 65±8 | N.E. |
| | PD 153035 | EGFR kinase | 97 | 12 | 91±20 | N.E. |
| | Erlotinib | EGFR kinase | 98 | 36 | 210±30 | N.E. |
| | Gefitinib | EGFR kinase | 91 | 5 | 380±40 | N.E. |
| | Lapatinib | EGFR kinase | 91 | 0 | 590±30 | N.E. |
| | GW 2974 | EGFR kinase | 89 | 18 | 1,300±500 | N.E. |
| | GW 583340 | EGFR kinase | 94 | 26 | 2,000±400 | N.E. |
| | Erbstatin analog | EGFR kinase | -24 | 2 | N.E. | N.E. * |
| Other confirmed granule formation inhibitors | ZM-306416 | VEGFR kinase | 97 | 21 | 670±200 | N.E. |
| | Camptothecin | Topoisomerase I | 81 | 40 | 720±100 | N.E. * |
| | PKC 412 | Pan-kinase inhibitor | 68 | 35 | 1,300±700 | N.E. * |
| | Aminopurvalanol A | CDKs | 62 | 40 | 910±400 | N.E. * |
| | 17-DMAG | Hsp90 | 92 | 33 | 29±3 | N.E. |
| Confirmed granule formation activators | Flurandrenolide | Corticosteroid | -165 | 7 | 23±20 | N.E. |
| | Beclomethasone | Corticosteroid | -116 | 16 | 42±7 | N.E. |
| | Ebastine | H1 receptor | -110 | 6 | 1,500±300 | N.E. |

N.E.: no effect.

* partial inhibition: a clear upper asymptote was not reached at the highest concentrations tested, or the upper asymptote did not reach 100% inhibition.

NIH-PA Author Manuscript NIH-PA Author Manuscript NIH-PA Author Manuscript



## Table 2

### Performance of 16 hits and erbstatin analog in the Alamar Blue viability assay

Summary assessment of the 16 hits and the erbstatin analog effects on the viability of A549-EGFRB, A549, H2030, H3255 and HCC4011 cell lines. The reported $IC_{50}$ values ±standard deviation were calculated based on dose response studies for each confirmed hit using the Alamar Blue viability assay as described under Materials and Methods.

| | | | Alamar Blue viability assay $IC_{50}$ (μM) | | | |
|---|---|---|---|---|---|---|
| | **Compound name** | **Molecular target** | **A549** | **H2030** | **H3255** | **HCC4011** |
| Known EGFR inhibitors | BIBU 1361 | EGFR kinase | 3.7±0.8* | 3.1±0.7* | 0.020±0.004 | 0.035±0.003 |
| | Tyrphostin AG 1478 | EGFR kinase | > 10 | > 10 | 0.049±0.001 | 0.033±0.007 |
| | PD 153035 | EGFR kinase | > 10 | > 10 | 0.072±0.012 | 0.048±0.012 |
| | Erlotinib | EGFR kinase | > 10 | > 10 | 0.045±0.005 | 0.048±0.006 |
| | Gefitinib | EGFR kinase | > 10 | > 10 | < 0.01 | 0.028±0.003 |
| | Lapatinib | EGFR kinase | > 10 | > 10* | 1.2±0.1 | 1.5±0.1 |
| | GW 2974 | EGFR kinase | > 10 | > 10 | 0.67±0.1 | 1.4±0.6* |
| | GW 583340 | EGFR kinase | > 10 | > 10 | 0.96±0.06 | 2.0±0.2 |
| | Erbstatin analog | EGFR kinase | > 10* | > 10* | > 10 | > 10* |
| Other confirmed granule formation inhibitors | ZM-306416 | VEGFR kinase | > 10 | > 10 | 0.09±0.007 | 0.072±0.01 |
| | Camptothecin | Topoisomerase I | 0.035±0.05 | 0.017±0.005 | 0.39±0.05 | 0.29±0.04 |
| | PKC 412 | Pan-kinase inhibitor | 0.34±0.03 | 2.0±1.7* | 1.9±0.2 | 2.3±0.6 |
| | Aminopurvalanol A | CDKs | > 10* | > 10* | > 10* | > 10* |
| | 17-DMAG | Hsp90 | < 0.01 | < 0.01 | 0.021±0.01* | 0.025±0.002* |
| Confirmed granule formation activators | Flurandrenolide | Corticosteroid | > 10 | > 10 | > 10 | > 10 |
| | Beclomethasone | Corticosteroid | > 10 | > 10 | > 10 | > 10 |
| | Ebastine | H1 receptor | > 10 | > 10 | > 10 | > 10 |

*partial inhibition: a clear upper asymptote was not reached at the highest concentrations tested, or the upper asymptote did not reach 100% inhibition.

NIH-PA Author Manuscript NIH-PA Author Manuscript NIH-PA Author Manuscript



*J Biomol Screen*. Author manuscript; available in PMC 2013 April 03.

**Table 3**

**Performance of 15 hits and erbstatin analog against a panel of kinases**

Summary assessment of the 16 hits and the erbstatin analog effects on the in-vitro enzymatic activities of EGFR, SRC, ABL, and VEGF1 kinases on the panel. The reported $IC_{50}$ values ±standard deviation were calculated based on dose response studies for each confirmed hit using the luminescence ADP kinase Glo assay as described under Materials and Methods.

| | | | Luminescence ADP kinase assay $IC_{50}$ (μM) | | | |
|---|---|---|---|---|---|---|
| | **Compound name** | **Molecular target** | **EGFR** | **SRC** | **ABL** | **VEGFR1** |
| Known EGFR inhibitors | BIBU 1361 | EGFR kinase | < 0.01 | > 10 | > 10 | > 10 |
| | Tyrphostin AG 1478 | EGFR kinase | < 0.01 | 2.6±1.3* | 2.0±0.6* | > 10* |
| | PD 153035 | EGFR kinase | < 0.01 | > 10 | 1.8±0.3* | > 10 |
| | Erlotinib | EGFR kinase | < 0.01 | 2.4±0.7* | 2.4±0.6* | 1.3±0.1* |
| | Gefitinib | EGFR kinase | < 0.01 | > 10 | > 10 | > 10 |
| | Lapatinib | EGFR kinase | 0.54±0.02 | > 10 | > 10 | > 10 |
| | GW 2974 | EGFR kinase | 0.12±0.03 | > 10 | > 10 | > 10 |
| | GW 583340 | EGFR kinase | 1.3±0.1 | > 10 | > 10 | > 10 |
| | Erbstatin analog | EGFR kinase | > 10 | > 10 | > 10 | > 10 |
| Other confirmed granule formation inhibitors | ZM-306416 | VEGFR kinase | < 0.01 | 0.33±0.08 | 1.3±0.2* | 0.33±0.04 |
| | Camptothecin | Topoisomerase I | > 10 | > 10 | > 10 | > 10 |
| | PKC 412 | Pan-kinase inhibitor | > 10* | > 10 | > 10 | > 10 |
| | Aminopurvalanol A | CDKs | > 10* | 0.12±0.02 | 1.5±0.5 | > 10 |
| Confirmed granule formation activators | Flurandrenolide | Corticosteroid | > 10 | > 10 | > 10 | > 10 |
| | Beclomethasone | Corticosteroid | > 10 | > 10 | > 10 | > 10 |
| | Ebastine | H1 receptor | > 10 | > 10 | > 10 | > 10 |

*partial inhibition: a clear upper asymptote was not reached at the highest concentrations tested, or the upper asymptote did not reach 100% inhibition.